THERMAL PERFORMANCE OF A POROUS RADIAL FIN WITH NATURAL CONVECTION AND RADIATIVE HEAT LOSSES

by

Mohammad Taghi DARVISHI[a], Rama Subba Reddy GORLA[b*], Farzad KHANI[a], and Abdul AZIZ[c]

[a] Department of Mathematics, Razi University, Kermanshah, Iran
[b] Department of Mechanical Engineering, Cleveland State University, Cleveland, O., USA
[c] Department of Mechanical Engineering, School of Engineering and Applied Science, Gonzaga University, Spokane, Wash., USA

Original scientific paper
DOI: 10.2298/TSCI120619149D

An analytic (series) solution is developed to describe the thermal performance of a porous radial fin with natural convection in the fluid saturating the fin and radiation heat loss from the top and bottom surfaces of the fin. The homotropy analysis method results for the temperature distribution and base heat flux are compared with the direct numerical results and found to be very accurate.

Key words: *porous radial fin, natural convection, radiation heat transfer, homotopy analysis method*

Introduction

In recent years, several novel ideas have been proposed for producing fins that are significantly lighter but have the thermal performance comparable to that of solid metallic fins. For example, pin fins made of polymer composites impregnated with carbon fibers give designers the flexibility to develop light weight sinks for the thermal management of electronic systems. Because of the large difference in the thermal conductivities of carbon fiber and polymer composite, such a fin exhibits strong orthotropic behavior requiring a two-dimensional heat conduction model for analysis as shown by Bahadur and Bar-Cohen [1], Zubair*, et al.* [2], and Aziz and Makinde [3]. Aziz and Rahman [4] considered a fin made of a functionally graded material and analyzed the performance of a radial fin with a continuously increasing thermal conductivity in the radial direction. Another innovative idea to enhance the performance of solid metal fin is to immerse the last 30% of the fin in a phase change material [5].

Many papers have explored the use of porous fins. Although a fin made of a porous material has low thermal conductivity, a very large area of the material comes in contact with the cooling fluid. This enables the porous fin to give superior performance with a significant reduction in weight compared with a solid metal fin. Kiwan [6] introduced the Darcy's model to write the energy equation governing the temperature distribution in the porous fin operating in a natural convection environment. The Darcy model simulates the fluid-solid interaction in the porous medium. He found that the thermal performance of a porous fin can be described by a single parameter *Sh* which is a combination of Rayleigh number, the Darcy number, the thermal conductivity ratio, *Kr,* and fin length to thickness ratio, *L/t.* He found that, with a

* Corresponding author; e-mail: r.gorla@yahoo. com

proper choice of *Kr* and *L/t,* the performance of a porous fin can exceed the performance of a solid fin. In a contemporaneous paper, Kiwan [7] extended the analysis to include the effect of radiative surface heat loss and concluded that at large Rayleigh numbers, radiation played a small role in the overall heat transfer process. In a subsequent paper, Kiwan and Zeitoun [8] performed a finite volume type numerical study to assess the performance of rectangular porous fins mounted around the inner cylinder of a cylindrical annulus. They found that under natural convection cooling porous fins enhanced the heat transfer rate by 75% compared with the corresponding value obtained with solid fins. Kim*, et al.* [9] investigated experimentally the impact of porous fins on the pressure drop and heat transfer characteristics of plate-fin heat exchangers. They tested porous fins made of 6106 aluminum-alloy foam with different permeabilities and porosities and concluded that porous fins of low porosity and high pore density are desirable for a compact heat exchanger design. Khaled [10] analyzed a porous rectangular fin with the cooling fluid flowing normal to the top face of the fin. Again he also found that permeable fins transfer more heat than solid fins at large values of dimensionless suction velocity and moderate holes-to-fin ratios. Kundu and Bhanja [11] developed an analytical procedure that allows the optimum dimensions of a porous fin to be established for a specified base heat transfer rate. Taklifi*, et al.* [12] studied the effect of MHD on the performance of a porous fin attached to a vertical surface. The use of porous metal fins to enhance condensation has been investigated by Shekarriz and Plumb [13] and Sarma and Mayinger [14] among others. Kahalerras and Targui [15] studied the performance of a double pipe heat exchanger fitted with porous fins. Tye-Gingras and Gosselin [16] used the evolutionary algorithms to minimize the thermal resistance of fin-and-porous-medium heat sink. The concept of thermal network combined with the basic fin theory was used by Jeng*, et al.* [17] to model forced convection over a porous heat sink. Naidu*, et al.* [18] reported a numerical study of natural convection from a cylindrical fin placed in a cylindrical porous enclosure.

Two recent works of immediate relevance to the present study are those of Maheria [19] and Gorla and Bakier [20]. Both these works derive a simple theoretical model to describe the temperature field in a single porous rectangular fin when it is losing heat by simultaneous natural convection and radiation to the surrounding fluid. The model is simple but does capture the essential features of the more elaborate model of Kiwan [6].

The preceding literature clearly shows the work on porous fins has been confined to straight fins of rectangular profile and pin fins. No attempt has been made to study porous radial fins although radial fins are used in numerous applications where porous fins can provide a lighter, cheaper, and superior alternative to solid metallic fins. The purpose of this paper is to use the simplified model proposed by Kiwan [6] and subsequently used by Maheria [19] and Gorla and Bakier [20] to analyze the thermal performance of radial porous fin of uniform thickness. The energy equation appears in the form of an ordinary differential equation containing two non-linear terms. The first non-linear term is associated with the buoyancy effects in the fluid and the permeability of the porous medium. The second non-linearity is a consequence of radiative cooling at the surface of the fin. Following [6, 19, 20], we assume the base of the fin at a constant temperature and the tip of the fin to be adiabatic. The present formulation characterizes the effect of ambient temperature differently from Maheria [19] and Gorla and Bakier [20] and provides a better picture of the effect of the ambient temperature on the thermal performance of the fin.

The method adopted to solve the non-linear problem analytically is the homotopy analysis method (HAM). The method was originally proposed by Liao [21]. Unlike other methods such as the perturbation method, HAM does not mandate the presence of small parameters in the mathematical model for it to work satisfactorily. The method can also be ele-

gantly combined with other analytical tools such as the Pade approximate which is a method of improving the convergence of the series The Pade approximate of a series such as HAM is the ratio of two polynomials, P of degree M and Q of degree N, whose coefficients are determined by imposing the condition that the expansion of the Pade approximate and the HAM series agree to the order $M + N$, and $Q(0) = 1$. Also, the method allows a convenient way of controlling and adjusting the convergence of the series [22]. These advantages are not available with other methods such as the variational iteration method [23], the generalized Taylor collocation method [24], finite difference and finite elements method [25], discrete Taylor series method [26], and others [27, 28].

Mathematical analysis

Consider a radial (annular or circular) fin of base radius r_b, tip radius r_t, and thickness t as illustrated in fig. (1). The base of the fin is maintained at a constant temperature T_b. The tip of the fin is assumed to be adiabatic. The fin is made of a porous material of effective thermal conductivity k_{eff} and permeability K. The fin is in contact with an ambient fluid which infiltrates through the fin following the Darcy's law. The fluid has a specific heat $c_{p,f}$, density ρ_f, kinematic viscosity v_f, thermal conductivity k_f, and coefficient of volumetric expansion β_f. The exposed surfaces (top and bottom) are assumed to gray with a constant emissivity ε and emit radiation to the ambient fluid (temperature T_b), which also serves as the radiation heat sink.

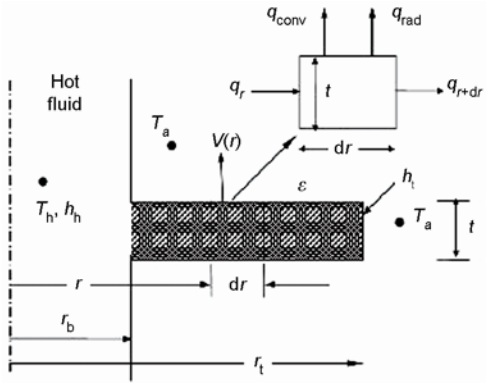

Figure 1. Porous radial fin geometry and energy balance

The assumptions are made in the derivation of the energy equation:

- the porous fin is homogeneous, isotropic and saturated with the single-phase ambient fluid,
- the thermophysical properties of both the solid matrix and the fluid are independent of temperature,
- the solid matrix and the fluid are in local thermodynamic equilibrium,
- heat conduction occurs only in the radial direction and consequently there are no transverse or circumferential temperature gradients in the fin,
- the solid-fluid interaction is described by the Darcy's law, and
- the fin operates under steady-state condition.

Making an energy balance on an element of fin (fig. 1) of circumference $2\pi r$, thickness t, and radial height dr, we get:

$$q_r - q_{r+dr} - q_{conv} - q_{rad} = 0 \tag{1}$$

where

$$q_r - q_{r+dr} = \frac{d}{dr}\left[k(2\pi rt)\frac{dT}{dr} \right] dr \tag{2}$$

$$q_{rad} = 2\varepsilon\sigma F_{f-a}(2\pi r dr)(T^4 - T_a^4) \tag{3}$$

$$q_{conv} = \rho_f v(r)(2\pi r dr)c_{p,f}(T - T_a) \tag{4}$$

where eq. 2 is based on the application of Fourier's law of heat conduction, eq. 3 is the radiative heat losses from the top and bottom faces of the fin, and eq. 4 is the rate of change of enthalpy of the buoyant fluid (infiltrate) passing through the fin. This is the rate at which the energy is removed from the fin by the buoyancy induced flow through the fin. The velocity of the buoyancy driven flow $v(r)$ at any radiation location r is obtained by applying the Darcy's law:

$$v(r) = \frac{g\beta(T - T_a)}{\nu_f} \tag{5}$$

Substituting eqs. (2)-(5) into eq. (1), leads to the non-linear ordinary differential equation governing the temperature distribution in the fin:

$$\frac{1}{r}\frac{d}{dr}\, r\, \frac{dT}{dr} - \frac{\rho_f g \beta_f K}{\nu_f k_{eff} t}(T - T_a) - \frac{2\varepsilon\sigma F_{f-a}}{k_{eff} t}(T^4 - T_a^4) = 0 \tag{6}$$

The boundary conditions at the fin's base and at the fin's tip may be written:

$$r = r_b, \quad T = T_b \tag{7}$$

$$r = r_t, \quad \frac{dT}{dr} = 0 \tag{8}$$

We introduce the dimensionless quantities:

$$\theta = \frac{T}{T_b}, \quad \theta_a = \frac{T_a}{T_b}, \quad R = \frac{r}{r_b}, \quad K_r = \frac{k_{eff}}{k_f}, \quad \mathrm{Da} = \frac{K}{t^2}, \quad \mathrm{Gr} = \frac{g\beta_f T_b t^3}{\nu_f^2} \tag{9}$$

$$\mathrm{Pr} = \frac{\nu_f}{\alpha_f}, \ \mathrm{Ra} = \mathrm{Gr}\ \mathrm{Pr}, \ Nc = \frac{\mathrm{Da}\ \mathrm{Ra}}{K_r}\left(\frac{r_b}{t}\right)^2 = \frac{\rho_f g K \beta_f c_{p,f} r_b^2 T_b}{\nu_f k_{eff} t}, \ Nr = \frac{2\varepsilon\sigma F_{f-a} r_b^2 T_b^3}{k_{eff} t} \tag{10}$$

and rewrite eqs. (6)-(8) in dimensionless form:

$$\frac{1}{R}\frac{d}{dR}\left(R\frac{d\theta}{dR}\right) - Nc(\theta - \theta_a)^2 - Nr(\theta^4 - \theta_a^4) = 0 \tag{11}$$

$$R = 1, \quad \Theta(R) = 1 \tag{12}$$

$$R = R^*, \quad \frac{d}{dR}\theta(R) = 0 \tag{13}$$

Equation (11) is a non-linear ordinary differential equation. It contains two non-linear terms. The first non-linearity is due to the natural convective transport of energy by the infiltrate. This energy is the rate at which the enthalpy of the infiltrate increases as it flows through the porous fin. The second non-linear term is associated with the surface radiative heat transfer from the fin to the ambient fluid which also serves as the radiation sink.

It may be noted that the parameter Nc is a combination of Darcy's number, Rayleigh number, the thermal conductivity ratio K_r, and the ratio of fin base radius to fin thickness. The parameter Nr indicates the role of surface radiation relative to conduction in the fin. The parameter Θ_a is the ratio of ambient fluid temperature and the base temperature. Equations (11)-(13) show that the temperature distribution in the fin depends on four dimensionless parameters Nc, Nr, Θ_a, and R^*.

The heat flow through the fin, q, can be found by applying the Fourier's law at the base of the fin:

$$q = -k_{\text{eff}}(2\pi r_{\text{b}} t)\left.\frac{\mathrm{d}T}{\mathrm{d}r}\right|_{r=r_{\text{b}}} \tag{14}$$

or dimensionless form:

$$Q = \frac{q}{2\pi k_{\text{eff}} t T_{\text{b}}} = -\theta'(1) \tag{15}$$

Homotopy analysis method

Let's define the (jointly continuous) map $\Theta(R; p) \mapsto \Theta(R)$, where the embedding parameter $p \in [0, 1]$, such that, as p increases from 0 to 1, $\Theta(R; p)$ vary from the initial guess to the exact solution $\Theta(R)$. To ensure this, we construct the following *zero-order deformation equation* of the governing equation:

$$(1 - p)\mathcal{L}[\Theta(R; p) - \theta_0(R)] = \hbar p \mathcal{N}[\Theta(R; p)] \tag{16}$$

where $\hbar \neq 0$ is a convergence-control parameter [22] which helps to ensure the convergence of the solution series; the operator $\mathcal{N}[\Theta(R; p)]$ is defined by the governing eq. (11) depending on the two-dimensional case. So $\mathcal{N}$ can be expressed by:

$$\mathcal{N}[\Theta(R; p)] := \frac{1}{R}\frac{\partial \Theta}{\partial R} + \frac{\partial^2 \Theta}{\partial R^2} - Nc(\Theta - \theta_a)^2 - Nr(\Theta^4 - \theta_a^4) \tag{17}$$

The boundary conditions (12) and (13) yields:

$$\Theta(1; p) = 1, \qquad \frac{\partial \Theta}{\partial X}(R^*; p) = 0 \tag{18}$$

$\mathcal{L}$ is the auxiliary linear operator defined by:

$$\mathcal{L}(\Theta) := \frac{\partial^2}{\partial R^2}\Theta \tag{19}$$

Clearly, when $p = 0$ the *zero-order deformation eqs.* (16) and (18) give rise to:

$$\Theta(R; 0) = \theta_0(R) \tag{20}$$

When $p = 1$, they become:

$$\Theta(R; 1) = \theta(R) \tag{21}$$

Here, $\Theta_0(R)$ is initial guess. We can assume the initial guess of $\theta(R)$ to be $\theta_0(R) = 1$.

Expanding $\Theta(R; p)$ in the Maclaurin series with respect to the embedding parameter p, we obtain:

$$\Theta(1; p) = \theta_0(R) + \sum_{k=1}^{\infty} \theta_k(R) p^k \tag{22}$$

where

$$\theta_k(R) = \frac{1}{k!}\frac{\partial^k}{\partial p^k}\Theta(R; 0) \tag{23}$$

Assuming that series converges at $p = 1$, we have:

$$\theta(R) = \theta_0(R) + \sum_{k=1}^{\infty} \theta_k(R) \tag{24}$$

Differentiating the *zero-order deformation eqs.* (16) and (18) m times with respect to p, then setting $p = 0$, and finally dividing by $m!$, we have the *high-order deformation equations* ($m \geq 1$):

$$\mathcal{L}[\theta_m - \chi_m \theta_{m-1}] = \hbar \mathcal{H}(R) \mathcal{K}_m \tag{25}$$

with the boundary conditions:

$$\theta_m(1) = 0, \qquad \theta'_m(R^*) = 0 \tag{26}$$

where

$$\chi_m = \begin{cases} 0, & m = 1 \\ 1, & m > 1 \end{cases} \tag{27}$$

and

$$\mathcal{K}_m = \frac{1}{R}\theta'_{m-1} + \theta''_{m-1} - Nc\left(\sum_{k=0}^{m-1} \theta_k \theta_{m-1-k} - 2\theta_{m-1}\theta_a\right) -$$
$$-Nr\left(\sum_{k=0}^{m-1} \theta_{m-1-k} \sum_{j=0}^{k} \theta_{k-1} \sum_{i=0}^{j} \theta_i \theta_{j-i}\right) + (1-\chi_m)(-Nc\theta_a^2 + Nr\theta_a^4) \tag{28}$$

where the prime denotes differentiation with respect to the similarity variable R. Then the solutions for eq. (25) can be expressed by:

$$\theta_m(R) = \chi_m \theta_{m-1}(R) + \hbar \mathcal{L}^{-1}[\mathcal{H}(R)\mathcal{K}_m] + c_1 R + c_2 \tag{29}$$

where the integral constants c_1 and c_2 are determined by boundary conditions (26) and $\mathcal{H}(R) = R$. Hence the m^{th}-order approximation of $\Theta(X)$ can be generally expressed by:

$$\theta_m(R) = \sum_{n=0}^{3m} \Gamma_{m,n}(\hbar) R^n \tag{30}$$

where $\Gamma_{m,n}(\hbar)$ are dependent upon $\hbar$. Equation (30) is a family of solutions which is expressed by the auxiliary parameter $\hbar$. With the aid of mathematical software, such as MATHEMATICA or MAPLE, it is easy to proceed to high orders. It is worth noting that until now, HAM has been applied to steady-state problems only. Whether or not it is applicable to transient problems *i. e.* partial differential equations awaits future research exploration. The computational time needed to implement HAM is comparable to the time needed for the direct numerical solutions but the real advantage of HAM is that it gives an analytical solution.

Results and discussion

It is important to ensure that the solution series (24) converges. Fortunately, we have the freedom to choose the values of the auxiliary parameters $\hbar$. This parameter provides a simple way to adjust and control the convergence region and as well as the rate of convergence of the series solution, as shown by Liao [21]. Let $\hbar$ be unknown variable. By plotting the curves of

Θ"(1) *vs.* $\hbar$, it is possible to choose the proper values of $\hbar$ so as to ensure that the series solution converges. A sample of these calculations is shown in figs. (2) and (3). The flat regions of the curves in figs. (2) and (3) establish the convergence region of the auxiliary parameter.

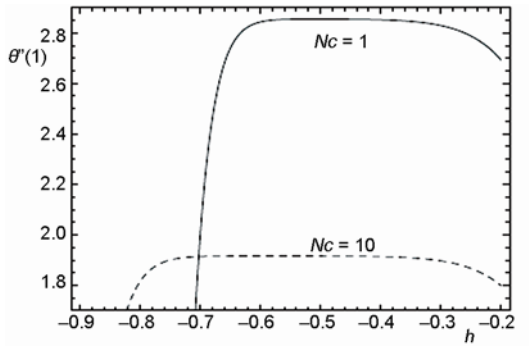

Figure 2. θ"(1) *vs.* $\hbar$ for the 20th-order approximation at $\Theta_a = 0.4$, $Nr = 1$, and $R^* = 1.5$

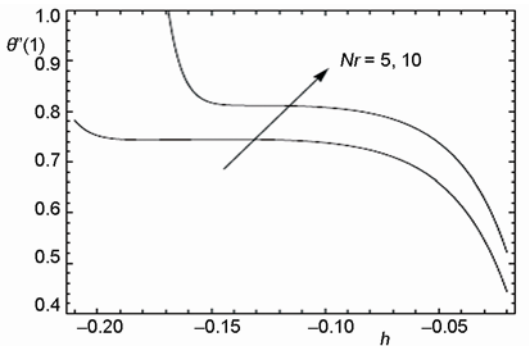

Figure 3. θ"(1) *vs.* $\hbar$ for the 20th-order approximation at $\Theta_a = 0.2$, $Nc = 1$, and $R^* = 2$

The HAM results were generated with the 20 terms of the series (24) and found to be in agreement with the direct numerical solution of eqs. (11)-(13) up to three places of decimal. The numerical solutions were obtained using MAPLE. The software uses a second-order difference scheme combined with an order bootstrap technique with mesh-refinement strategies: the difference scheme is based on either the trapezoid or midpoint rules; the order improvement/accuracy enhancement is either Richardson extrapolation or a method of deferred corrections.

Figure (4) shows the effect of natural convective heat loss on the temperature distribution in the fin when the radiation heat loss, the environment temperature, and the ratio of outer to inner radius are kept fixed. As the buoyancy effects become stronger *i. e*. *Nc* increases, the local temperature in the fin decreases. This behavior is synonymous with the well-known behavior of the solid radial fin. The decrease in the local temperature is accompanied by the increase in the base heat flow as will be seen later. The parameter *Nc* represents the buoyancy effect. Buoyancy is principally a macro scale effect. The buoyancy force influences the velocity and temperature fields. The parameter *Nr* represents radiation effect. It influences the temperature field by increasing the heat transfer rates from the surface. When the convection parameter *Nc* and the radiation parameter *Nr* is allowed to vary as in fig. (5), the local fin

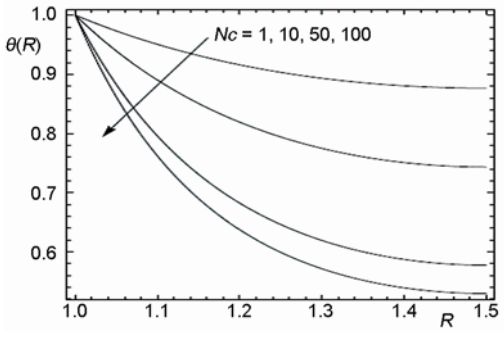

Figure 4. Analytic temperature distributions for the 20th-order HAM approximation at $\theta_a = 0.4$, $Nr = 1$, and $R^* = 1.5$, for different values of *Nc*

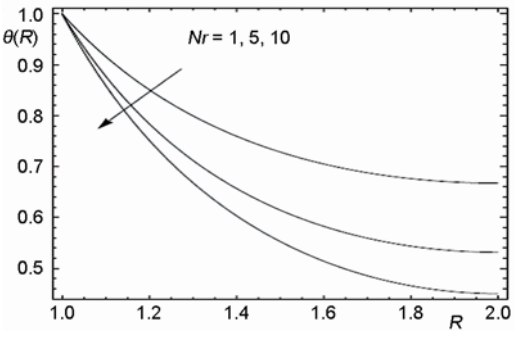

Figure 5. Analytic temperature distributions for the 20th-order HAM approximation at $\theta_a = 0.2$, $Nc = 1$, and $R^* = 2$, for different values of *Nr*

temperature decreases because of the increasing strength of radiative heat exchange between the exposed surface of the fin and the ambient.

Figure (6) shows that as the ambient temperature decreases, it causes the local fin temperature to decrease. This indicates augmented heat transfer rates. These results pertain to the circumstance when the buoyancy induced natural convection is much stronger *(Nc* =10) than the surface radiation transport (*Nr* = 1). The quantity of more practical importance is the heat flow through the base of the fin, $-\theta'(1)$, given by eq. (15). The results are in figs. (7)-(10) and cover a wide range of values of the parameters *Nc, Nr,* and θ_a for fin geometries with R^* = 1.75 and 2.0. These values of R^* are often used to design the cooling fins attached to the cylindrical surfaces of combustion chambers and for improving the heat dissipation from the gas-side of the heat exchanger tubes. The results in figs. (7)-(10) confirm the expectation that as the natural convection and radiation effects increase in strength either individually or in concert, the base heat flow increases. Figures (7) and (8) show that heat transfer rates get augmented as a result of increased buoyancy force. Figures (9) and (10) show that heat transfer rates get augmented as a result of increased emissivity of the surface. We believe the results presented in figs. (7)-(10) can be used to evaluate the thermal performance of porous ra-

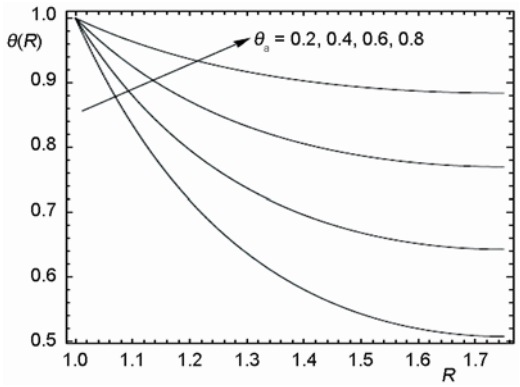

Figure 6. Analytic temperature distributions for the 20th-order HAM approximation at *Nr* = 1, *Nc* = 10, and *R = 1.75, for different values of θ_a**

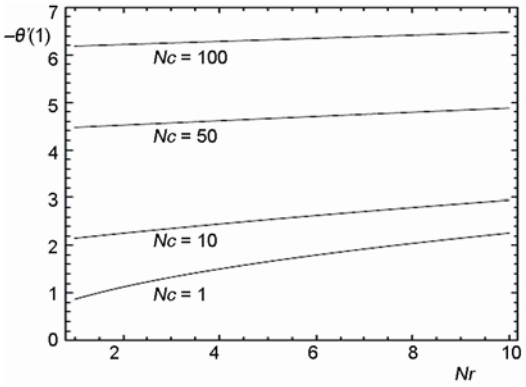

Figure 7. Dimensionless base heat flow: effect of natural convection and radiation when θ_a = 0.2, and *R = 1.75**

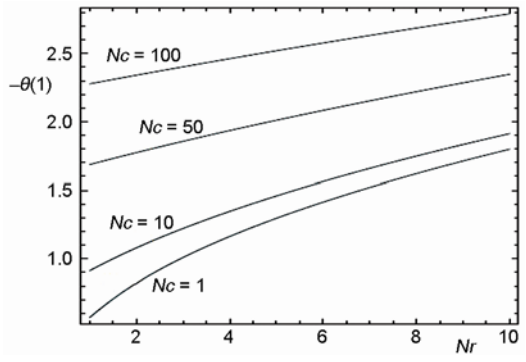

Figure 8. Dimensionless base heat flow: effect of natural convection and radiation when θ_a = 0.6, and *R = 1.75**

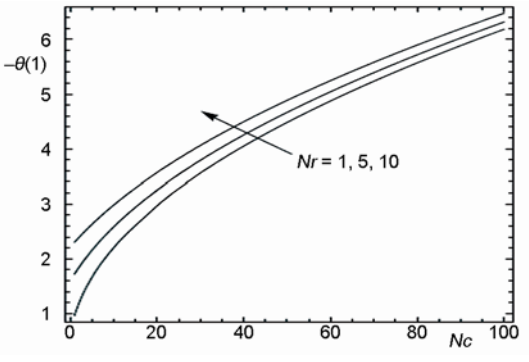

Figure 9. Dimensionless base heat flow: effect of natural convection and radiation when θ_a = 0.2, and *R = 2**

dial fins under a variety of operational conditions. Figure (11) displays heat transfer rates *vs.* ambient temperature with the ratio of tip radius to base radius (R^*) as a parameter. We observe that the heat transfer rates increase with R^*. This is due to the increased heat transfer area as R^* increases. As the ambient temperature increases the heat transfer rate decreases. This is to be expected because the driving force for heat transfer rate decreases as Θ_a increases.

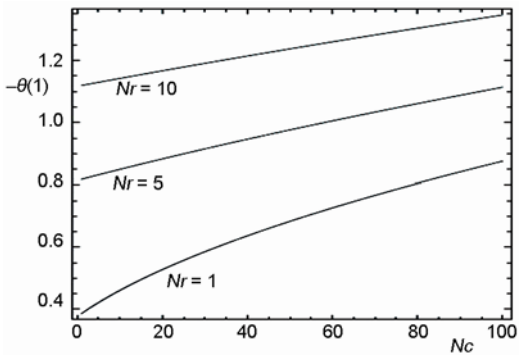

Figure 10. Dimensionless base heat flow: effect of natural convection and radiation when Θ_a = 0.8, and R^* = 2

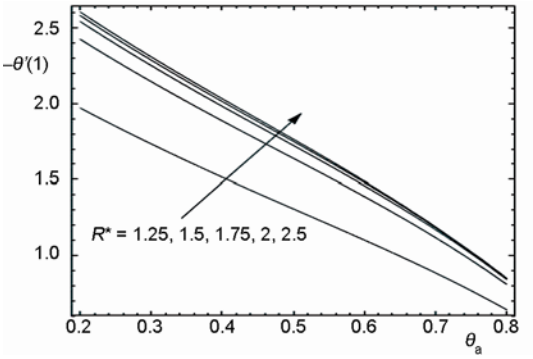

Figure 11. Dimensionless base heat flow: effect of fin radial parameter and ambient temperature when Nc = 10, and Nr = 5

Nomenclature

$c_{p,f}$ – specific heat of the ambient fluid, [Jkg^{-1}]
Da – Darcy number, [–]
F_{f-a} – shape factor for radiation heat transfer, [–]
g – acceleration due to gravity, [ms^{-2}]
K_r – thermal conductivity ratio, [–]
k_{eff} – effective thermal conductivity of porous fin, [Wm^{-1}K^{-1}]
k_f – thermal conductivity of ambient fluid, [Wm^{-1}K^{-1}]
L – length of the fin, [m]
Nc – buoyancy or natural convection parameter, [–]
Nr – radiation parameter
p – embedding parameter, [–]
Q – dimensionless base heat flow, [–]
q – base heat flow, [Wm^{-2}]
R – dimensionless radius, [–]
R^* – ratio of tip radius to base radius, [–]
r – radial co-ordinate, [m]
r_b – base radius, [m]
r_t – tip radius, [m]
T – local fin temperature, [K]
T_a – ambient temperature, [K]
T_b – base temperature, [K]
t – fin thickness, [m]
$\hbar$ – auxiliary parameter, [–]
$\mathcal{L}$ – auxiliary linear operator
$\mathcal{N}$ – non-linear operator

Greek symbols

α_f – thermal diffusivity of ambient fluid, [m^{2}s^{-1}]
β_f – volumetric thermal expansion coefficient of the ambient fluid, [m^{2}K^{-1}]
ε – surface emissivity of fin, [–]
θ – non-dimensional temperature, [–]
θ_a – dimensionless ambient temperature, [–]
θ_m – mth-order approximation, [–]
ν_f – kinematic viscosity of the ambient fluid, [m^{2}s^{-1}]
ρ_f – density of the ambient fluid, [kgm^{-3}]
σ – Stefan-Boltzmann constant, [Wm^{-2}K^{-4}]
χ_m – two-valued function, [–]

References

[1] Bahadur, R., Bar-Cohen, A., Orthotropic Thermal Conductivity Effect on Cylindrical Pin Fin Heat Transfer, *Int. J. Heat Mass Transfer, 50* (2007), 5-6, pp. 1155-1162
[2] Zubair, S. M., *et al.*, Thermal Analysis and Optimization of Orthotropic Pin Fins: A Closed-Form Analytical Solution, *ASME J Heat Transfer, 132* (2010), 031301-1
[3] Aziz, A., Makinde, O. D., Heat Transfer and Entropy Generation in a Two-Dimensional Orthotropic Convection Pin Fin, *Int. J. Exergy, 7* (2010), 5, pp. 579-592

[4] Aziz, A., Rahman, M. M., Thermal Performance of a Functionally Graded Radial Fin, *Int. J. Thermophysics, 30* (2009) 5, pp. 1637-1648
[5] Krishnan, S., *et al.*, A Novel Hybrid Heat Sink Using Phase Change Materials for Transient Thermal Management of Electronics, *IEEE Trans. Compon. Packag. Technol., 28* (2005), 2, pp. 281-289
[6] Kiwan, S., Thermal Analysis of Natural Convection in Porous Fins, *Transport in Porous Media, 67* (2006), 1, pp. 17-29
[7] Kiwan, S., Effect of Radiative Losses on Heat Transfer from Porous Fins, *Int. J. Thermal Sci., 46* (2007), 10, pp. 1046-1055
[8] Kiwan, S. Zeitoun, O., Natural Convection in a Horizontal Cylindrical Annulus Using Porous Fins, *Int. J. Numer. Method H., 18* (2008), 5, pp. 618-634
[9] Kim, S. Y. *et al.*, Flow and Heat Transfer Correlations for Porous Fin in a Plate-Fin Heat Exchanger, *ASME J. Heat Transfer, 122* (2000), 3, pp. 572-578
[10] Khalid, A. R. A., Investigation of Heat Transfer Enhancement through Porous Fins, *ASME J. Heat Transfer, 132* (2010), 034503-1-5
[11] Kundu, B., Bhanja, D., An Analytical Prediction for Performance and Optimum Design Analysis of Porous Fins, *Int. J. Refrigeration, 34* (2011), 1, pp. 337-352
[12] Taklifi, A., *et al.*, The Effect of MHD on a Porous Fin Attached to a vertical isothermal Surface, *Transport in Porous Media, 85* (2010), 1, pp. 215-231
[13] Shekarriz, A. Plumb, O. A., Enhancement of Film Condensation Using Porous Fins, *J. of Thermo. Phys. Heat Transfer, 3* (1989), 3, pp. 309-314
[14] Sarma, P. K. Mayinger, F., Condensation on Vertical Porous Metal Fins, *The Canadian J. Chem. Engr., 70* (1992), 3, pp. 463-469
[15] Kahalerras, H., Targui, N., Numerical Analysis of Heat Transfer Enhancement in a Double Pipe Heat Exchanger with Porous Fins, *Int. J. Numerical Methods H., 18* (2008), 5, pp. 593-617
[16] Tye-Gingras, M. Gosselin, L., Thermal Resistance Minimization of a Fin-and-Porous-Medium Heat Sink with Evolutionary Algorithms, *Numerical Heat Transfer: Part A - Applications, 54* (2008), 4, pp. 349-366
[17] Jeng, T.-M, *et al.*, An Analytical Study of Local Thermal Equilibrium in Porous Heat Sinks Using Fin Theory, *Int. J. Heat Mass Transfer, 49* (2006), 11, pp. 1907-1914
[18] Naidu, S. V., *et al.*, Performance of a Circular Pin Fin in a Cylindrical Porous Enclosure, *Int. Comm. Heat Mass Transfer, 31* (2004), 8, pp. 1209-1218
[19] Maheria, M. G., Thermal Analysis of Natural Convection and Radiation in Porous Fins, M. Sc. thesis, Cleveland State University, O., USA, 2010
[20] Gorla, R. S. R., Bekier, A. Y., Thermal Analysis of Natural Convection and Radiation in Porous Fins, *Int. Comm. Heat Mass Transfer, 38* (2011), 5, pp. 638-645
[21] Liao, S. J., *Beyond Perturbation: Introduction to the Homotopy Analysis Method,* Chapman & Hall/CRC Press, Boca Raton, Fla., USA, 2003
[22] Liao, S. J., Notes on the Homotopy Analysis Method: some Definitions and Theorems, *Commun. Nonlinear. Sci. Numer. Simulat., 14* (2009), 4, pp. 983-997
[23] Biazar, J., *et al*., Variational Iteration Method for Solving FokkerPlanck Equation, *Journal of the Franklin Institute, 347* (2010), 7, pp. 1137-1147
[24] Cenesiz, Y., *et al*., The Solution of the BagleyTorvik Equation with the Generalized Taylor Collocation Method, *Journal of the Franklin Institute, 347* (2010), 2, pp. 452-466
[25] Kitahara, N., *et al.*, Approximate Solutions for Axisymmetric Exterior-Field Problems by the Combined Scheme of Finite Elements and Finite Differences, *Journal of the Franklin Institute, 328* (1991), 2-3, pp. 217-229
[26] Jacobsohn, G., A Discrete Taylor Series Method for the Solution of Two-Point Boundary-Value Problems, *Journal of the Franklin Institute, 338* (2001), 1, pp. 61-68
[27] Ebadi, G., Biswas, A., Application of the G'/G-Expansion Method for non-Linear Diffusion Equations with non-Linear Source, *Journal of the Franklin Institute, 347* (2010), 7, pp. 1391-1398
[28] Shang, X., *et al*., An Efficient Method for Solving Emden Fowler Equations, *Journal of the Franklin Institute, 346* (2009), 9, pp. 889-897

Paper submitted: June 19, 2012
Paper revised: July 19, 2012
Paper accepted: July 26, 2012